Leak detection of water supply networks using error-domain model falsification

Gaudenz Moser[1], Stephanie German Paal[2] and Ian F.C. Smith[1]

(1) Applied Computing and Mechanics Laboratory (IMAC)

School of Architecture, Civil and Environmental Engineering (ENAC)

Swiss Federal Institute of Technology (EPFL)

Lausanne, Switzerland

(2) Zachry Department of Civil Engineering, College of Engineering

Texas A&M University

College Station, Texas, USA

Abstract

Pressurized fresh-water fluid-distribution networks are key strategic infrastructure elements. On average, 20% of water is lost by way of leaks around the world. This illustrates the need for more efficient management of pressurized fluid-distribution networks. This paper presents a system identification methodology known as error-domain model falsification adapted for performance assessment of water distribution networks and more specifically, to detect leak regions in these networks. In addition, a methodology to approximate the demand at nodes in water-supply networks is presented and a methodology for estimating uncertainties through experimentation is described. The use of error-domain model falsification for practical use in water distribution networks shows great potential. Finally, two case studies are presented. The first case study is from the water-distribution network of the city of Lausanne. An experimental campaign was carried out on this network to simulate leaks by opening hydrants. The second case study is from a water-distribution network of the commune of Bagnes, and a leak scenario was evaluated. These two case studies illustrate, using full-scale measurements, the potential of error-domain model falsification for the performance assessment of water-distribution networks.

Introduction

Annually, 184 billion USD are spent on clean water supply worldwide. However, collectively, water utilities lose an estimated 9.6 billion USD each year due to water leakage (Sensus 2012). Water supply networks lose an average of 20% of their water supply (Figure 1). The Sensus report also includes an estimate that if leaks were reduced by 5% and pipe bursts by 10%, utilities could save up to 4.6 billion USD.

Currently, most utilities react to leakage on an ad-hoc basis, responding to leaks and bursts and repairing infrastructure only as required by leakage events. There is a need for more rational and systematic strategies for managing infrastructure. Monitoring of water-supply networks could support this need and sensor-based diagnostic methodologies have the potential to provide enhanced management support.

Detecting leaks in water distribution networks is not a new challenge. Several studies over the past century have involved leak detection in fresh-water supply-networks. Hope (1892) studied water losses, and Babbitt et al. (1920) described examples of leak-detection methods such as visual observation and sounding through the soil with a steel rod. Water-hammer techniques and acoustic measurements, considered to be more advanced leak detection techniques, have also been developed. In addition, water loss and related costs have been highlighted for many decades (Niemeyer 1940; Johnson 1947).

Studies involving various leak-detection methodologies have continued into this century. Leak-noise correlation (Grunwell and Ratcliffe 1981; Gao et al. 2006; 2009), pig-mounted acoustic sensing (Mergelas and Henrich 2005) (a "pig" is a device used for cleaning and inspecting pipelines) and ground penetrating radar (Demirci et al. 2012) have all been studied. These techniques are not appropriate for monitoring large networks due to high costs. However, these methods are useful as complements to other methods in order to, for example, locate leaks in network segments that have already been identified to contain leaks.

An additional method, termed water balance, where the network is audited in order to examine the equality between water placed into the distribution system and water taken out was developed by Lambert and Hirner (2000). Morrison created the night flow district metered area (DMA) method (2004). In this method, the network is separated into segments and the water that flows in and out of these segments is metered. Water loss is estimated by taking these measurements when the demand is minimal, usually at night.

61　In addition, there are several transient-based techniques which use pressure measurements to

62　detect leaks in water supply networks by measuring transient signals. Colombo et al. (2009)

63　reviewed these types of methods and established three sub-categories: inverse-transient analysis

64　(Vitkovsky et al. 2000; 2007), direct transient analysis (Whittle et al. 2010; 2013; Srirangarajan

65　et al. 2010) and frequency-domain techniques. The accuracy of the results is affected by the

66　uncertainties associated with these systems. Thus, many of these techniques are used on single,

67　underground pipelines (Puust et al. 2010) rather than complex water distribution networks. An

68　exception is the study presented by Whittle et al. (2013). However, in this case, slow leak

69　development requires the use of other detection methods.

70　Another class of techniques are those based on comparisons of measurements with predictions

71　obtained from hydraulic models. This challenge is often framed as an optimization task. The

72　goal is to minimize the differences between predicted values from flow models and network

73　measurements. Such techniques are often based on minimization of least-squares (Pudar and

74　Liggett 1992; Andersen and Powell 2000). Mounce et al. (2009; 2011) used machine learning

75　and fuzzy inference to detect leaks.

76　Poulakis et al. (2003) proposed a Bayesian system-identification methodology for leakage

77　detection. Rougier (2005), Puust et al. (2006) and Barandouzi et al. (2012) also proposed Bayes-

78　based leak detection methodologies. Romano et al. (2012; 2013; 2014) implemented Bayesian

79　inference in a pipe burst detection framework. Hypotheses made when using traditional residual

80　minimization or Bayesian inference techniques are usually impossible to meet due to the

81　presence of systematic modelling errors and unknown values of induced correlations (Goulet

82　and Smith 2013).

83　Leak detection is not uniquely carried out in fresh-water-distribution networks. Other

84　pressurized fluid-distribution systems such as oil and gas pipelines may also be subject to leaks.

85　In such cases, the consequences of a leak may be dangerous with a risk of environmental

86　pollution. The Alaska Department of Environmental Conservation (ADEC 1999) presented a

87　review of leak-detection technologies for crude oil-transmission pipelines. For gas pipelines,

88　Murvay and Silea (2012) surveyed leak detection and localization techniques. The techniques

89　presented in these references are comparable to those developed for fresh-water networks. The

90　main difference is the presence of closely-coupled segments in the water network compared

91　with pipelines.

92   Robert-Nicoud et al. (2005) developed a methodology for sequential sensor placement in water

93   supply networks using entropy. Similarly, Goulet and Smith (2012) developed a model

94   falsification method called error domain model falsification for bridge diagnosis. In addition,

95   they carried out a preliminary study using this method for leak detection on a water supply

96   network (Goulet et al. 2013). This study showed good results for leaks of 100 l/min which is

97   not adequate for full-scale applications; practitioners are interested in detecting much smaller

98   leaks. Moser and Smith (2015) presented a methodology for reduction of water supply networks

99   when paired with error-domain model falsification for leak detection. The reduction process

100 translates the network model into a simpler equivalent model (reducing the number of nodes

101 and connections, and in turn, calculations). Further, Moser et al. (2016a,b) extended this work

102 to electrical networks in order to provide additional case studies for leak detection in water

103 supply networks as the two network types are analogous. In short, previous work has focused

104 on the development of individual technical aspects of the leak detection methodology. What

105 remains is a need to evaluate the performance of these individual aspects as a combined

106 methodology in real-world scenarios. This paper presents the complete scheme with practical

107 case studies that involve real measurements at various leak intensities.

108 Measurements are not useful unless the data that is generated can be interpreted appropriately.

109 This paper presents a methodology that accommodates systematic uncertainties and is robust in

110 the presence of unrecognized correlations. The objective is to provide a general diagnostic

111 methodology – for water distribution networks, and more generally, for pressurized fluid

112 distribution networks – that is able to locate leak regions. The methodology results in a

113 designated area, or areas, where a leak is known to be present. The size of the region, as well

114 as the number of regions, depends on the number of sensors that are used and the available prior

115 knowledge of the system.

116 In the following section, the diagnosis methodology is described in more detail. It is then

117 described how this methodology has been modified to support leak detection in water supply

118 networks. The usefulness of the methodology through an application to a part of the city of

119 Lausanne water distribution network is illustrated. In this application, fire hydrants have been

120 opened to simulate leaks. Leak region detection, as well as an estimation of the demand and

121 associated uncertainties is presented. Finally, a discussion of the more general impact of this

122 work is presented.

123   **Methodology**

124   Over nearly twenty years, several researchers have contributed to a methodology for diagnosis
125   called error-domain model falsification (Smith 2016). This methodology is most useful in cases
126   where little information is available to describe the relationships between uncertainties at
127   locations where measurements and predictions are compared. The methodology uses explicit
128   representations of modelling and measurement uncertainty distributions at each location
129   (Goulet and Smith 2012; Pasquier and Smith 2015). Prior knowledge is used to define bounds
130   for the parameter values and to build sets of possible scenarios. A scenario corresponds to a set
131   of parameter values describing the state of the system (e.g. a leak location). Scenarios are
132   generated in order to cover the range of all possible states of the system.

133   As shown in Equation 1, when comparing predictions g_i from a numerical model with a
134   measurement, y, modelling uncertainty ($u_{modelling}$) and the measurement uncertainty
135   ($u_{measurement}$) have to be included (Goulet and Smith 2013).

$$g_i + u_{modelling} = Reality = y + u_{measurement} \qquad (1)$$

136   Equation 1 can be rearranged to obtain Equation 2 in which both uncertainties are combined.

$$g_i - y_{sim}(t_j) = u_{measurement} - u_{modelling} = u_{combined} \qquad (2)$$

137   Using this combined uncertainty ($u_{combined}$), threshold bounds (T_{low}, T_{high}) are computed
138   (by taking the 95 % interval of the probability density function). The threshold bounds are used
139   in Equation 3 to determine if the predictions are close enough to the measurements at each
140   measurement location.

$$T_{low} \leq g_i - y \leq T_{high} \qquad (3)$$

141    $$where\ g_i = g(\theta_{i1}, ..., \theta_{ik})$$

142   Figure 2 shows the steps of error-domain model falsification. The first step is to define
143   scenarios. The scenarios, s_i are defined by the parameters θ_{ik} that need to be identified. For
144   example, in the case of leak detection, the parameters are leak locations and leak intensity. The
145   scenarios are generated by sampling to cover all the possible behaviors of the system. Some
146   expert input can also be useful to reduce the sampling size. They are then simulated through a
147   numerical model of the system in order to obtain a population of model predictions (termed the

148   initial model set). These predictions are used for the identification by comparing them with

149   measurements.

150   The distinction has to be made between physical and simulated measurements. Simulated

151   measurements are necessary in order to estimate the performance of sensor configurations prior

152   to physical measurement. Simulated measurements are obtained by randomly taking a model

153   instance in the initial model set and adding the combined uncertainties (modelling and

154   measurement) to predictions. Measurements are obtained from the sensors on the real/physical

155   network.

156   For real and simulated cases, measurements are compared with predictions for each model

157   instance. Threshold bounds, see Equation 3, are used to identify model instances that are

158   compatible with the measurements (candidate models). If the difference between the predictions

159   and the measurements (real or simulated) is within the bounds defined by the thresholds, then

160   the model instance is accepted to be part of the candidate model set. Otherwise, the model

161   instance is falsified and removed from the candidate model set.

162   Expected identifiability is a cumulative distribution function (CDF) that represents the

163   probabilities associated with obtaining a specific number of candidate models. This CDF is

164   built by testing a large number of simulated leaks on the network. For each scenario, the number

165   of candidate scenarios is computed using the error-domain model falsification procedure

166   presented above. This measure indicates the performance of the diagnosis and is used

167   throughout the work presented here.

168   *Uncertainties*

169   The task of estimating correct values for uncertainties is challenging. Sometimes, the

170   information can be determined experimentally (for example, for the sensors). Indications of

171   other uncertainties can be found in the literature. Model simplification uncertainty values are

172   more difficult to estimate. In the case of water distribution networks, estimation of the

173   uncertainty of the demand is challenging, particularly when it is modelled using a statistical

174   distribution and when there is limited data to justify assumptions. The performance of

175   identification using error-domain model falsification is dependent on the estimation of

176   uncertainties. An overestimation of uncertainties will lead to poor identification performance.

177   In extreme cases, either all model instances are accepted because they are all within the range

178   of the thresholds or all model instances are rejected. An incorrect estimation of the uncertainty

179 (or a wrong hypothesis in the modelling) can lead to an incorrect diagnosis. The methodology

180 created here uses experimental data to obtain an estimation of the threshold values, and, thus

181 the combined uncertainties.

182 The threshold bounds used in error-domain model falsification to falsify model instances are

183 computed by combining uncertainties that are representative of modelling and measurement

184 errors. Measurement errors are mainly due to sensor resolution since noise and sensor bias can

185 be considered to be negligible. Modelling errors are due to model simplifications and to errors

186 associated with model parameters. Model parameters are often not exactly known. They are

187 based on the network-design plans and estimations. Sometimes, parameters are estimated based

188 on hypotheses made using engineering experience.

189 Model parameters are categorized into two groups. The first group contains the primary

190 parameters which characterize leak scenarios. For leak detection, these are the leak position and

191 leak intensity, as described above. The other parameters, called secondary parameters, do not

192 explicitly characterize the scenarios. The uncertainties associated with these parameters are

193 included in the combined uncertainty that is used to estimate the threshold bounds.

194 Secondary parameters include: pipe diameter, pipe roughness, pipe length, nodal demand, node

195 elevation, and the water level in the tank. The propagation of uncertainties of secondary

196 parameters through the model is computed using the Monte-Carlo method. Thousands (10,000)

197 of simulations are carried out by varying the parameters following the uncertainty distributions.

198 An example of a choice of uncertainties is given in Table 1. Three distributions, exponential

199 (Exp), normal (N) and uniform (U) are used. The arguments of these distributions contain

200 defining parameters.

201 The demand at each node is estimated using an exponential law. The mean of the exponential

202 law (3.13 l/min) represents the minimal demand ratio. Minimal demand ratio is the minimal

203 consumption divided by the number of nodes. By making this hypothesis, the assumption is

204 made that each node has the same "weight". There is no distinction between large and small

205 consumers; it is the simplest way of modelling the demand without any prior knowledge. For

206 the node elevation and pipe diameter, the uncertainties are represented by a zero-mean normal

207 distributions with standard deviations of 15 cm and 0.75 mm, respectively. These values have

208 been estimated using engineering judgement. Pipe length uncertainty is described by a uniform

209 distribution with minimum and maximum values taken from an ISO norm (ISO 2531 2009).

210   The values for the pipe roughness and the tank level have been estimated by a review of

211   statistical variation of these data.

212   Using these uncertainty values, a sensitivity study has been carried out. The relative importance

213   of each parameter is estimated using the surface response technique (Fang et al. 2005; Box and

214   Draper 1959). The technique involves approximating the numerical model by a linear model

215     $\mathbf{Y} \approx \mathbf{M\beta}$ where $\mathbf{Y}$ is the vector of predicted values and $\mathbf{M}$ the model matrix built from the

216   standardized parameters. The vector $\mathbf{\beta}$ is the least-square estimator of the parameter vector.

217   Each element of this vector represented the relative importance of the associated parameter.

218   Results are given in Table 2. This table gives the relative importance of the uncertainties in the

219   computation of the flow predictions and pressure predictions for each parameter. One

220   uncertainty has a much larger impact than the others—the uncertainty on the nodal demand,

221   with more than 99% relative importance. These results show that when the demand is not well

222   known and an exponential law is used to model it, the uncertainty of the demand dominates the

223   uncertainties of the other parameters. In such situations, the uncertainty of the nodal demand

224   can be considered alone to represent the uncertainty of the secondary parameters.

225   Estimation of threshold values

226   The overall concept of this methodology is to infer threshold values using measurements that

227   represent known events. Instead of searching unknown leaks, the goal is to start with created

228   leaks. Such experiments can be carried out on a network by opening hydrants and controlling

229   the outcome (flow).

230   When the leak intensity and its location is known with certainty, remaining sources of

231   uncertainty can be quantified. The difference between predictions of this scenario and the

232   measurements is computed. This difference is then taken to be the combined uncertainty of

233   modelling and measurement errors. By repeating these operations for a range of measurements

234   and various scenarios, knowledge of uncertainties is increased. This process is illustrated in

235   Figure 3.

236   This methodology has been adapted for two desired quantities in water-supply management:

237   (1) leak region detection; and (2) demand estimation. The two EDMF-based methodologies are

238   described in further detail in the following sections, followed by a discussion of two case studies

239   in these approaches using sections of real water supply networks in the city of Lausanne and

240   commune of Bagnes.

241   *Leak-region detection*

242   For leak region detection, numerical simulations are performed using the water distribution

243   network simulation software EPANET (Rossman 2000). The goal is to develop a methodology

244   that is capable of identifying and defining areas where a leak is located. The size of leak regions,

245   is dependent on the number of sensors used for identification and the prior knowledge of the

246   system.

247   Leak scenarios

248   In order to detect a leak, a set of candidate model instances is built using leak scenarios. For

249   this study, scenarios are constructed following two hypotheses: (1) one leak occurs at a time;

250   and, (2) leaks occur at a node in the network model. The configurations are obtained by varying

251   leak position (the node where the leak occurs) and leak intensity (the flow going out through

252   the node), see Figure 4. The number of scenarios is equal to the number of nodes multiplied by

253   the number of intensities that are considered. It is not necessary to model leaks that occur at

254   intermediate points of pipes since the presence of uncertainties means that only leak regions,

255   which are bounded by nodes, are identified. Intermediate points do not influence the size of the

256   leak region.

257   The leak scenarios are simulated using EPANET to obtain a population of model instances. The

258   simulations are steady-state only (not transient). For each model instance, predicted values are

259   computed for the physical quantities (flow or pressure) that are measured by sensors on the

260   network. These predictions are then compared with measurements in the error-domain model-

261   falsification process.

262   Comparison with simulated measurements

263   This section presents results that have been obtained through a study carried out on part of the

264   fresh-water distribution network in Lausanne, Switzerland. This network contains 263 nodes

265   and 295 pipes. For illustration, in this part of the study, simulated measurements are used (a

266   later section includes two case studies where full-scale measurements are employed).

267   Simulations of measurements and leak scenarios are performed based on the minimum water

268   demand. Analysis of water distribution networks is generally conducted during minimum

269   demand hours because uncertainties related to the consumption is minimal in this time period.

270   In this case, this minimal demand is 830 l/min. This value was then divided by the number of

271   nodes to obtain the mean consumption for each node. For simulations, the nodal demand is

272   described by an exponential distribution. The exponential distribution is utilized as a logical

273   way to represent this water demand where there is a high probability to have a low consumption

274   and a low probability to have a high consumption.

275   For this illustration, the number of sensors is chosen to be three, and they were placed using a

276   greedy algorithm (Moser et al. 2016a). Figure 5 shows the results obtained for four leak

277   scenarios. White circles indicate the demand nodes. The links between these nodes are the

278   pipes. Squares are sensor locations on the network. The cross gives the position of the simulated

279   leak. In each of these four examples, the leak intensity used is 100 l/min. The nodes in dark

280   grey indicate the candidate leak scenarios, i.e. those possibilities that have not been falsified.

281   The four examples in Figure 5 illustrate two situations. First, in Cases (1) and (2), the number

282   of candidate scenarios is important. The size of the regions that are defined by the candidate

283   leak scenarios is too large to be able to satisfactorily identify the leak-region. These results

284   show that the methodology may be useful only to falsify one side of the network. In Case (1)

285   all candidate leak scenarios on the right side have been eliminated, and in Case (2) the entire

286   left side is falsified. These results may be useful in practice if the methodology is combined

287   with local leak detection techniques, such as acoustic methods. Discarding half of the leak

288   locations divides the necessary time for searching with a local technique in half. Nevertheless,

289   more accuracy is desirable. In Cases (3) and (4) the number of candidate leak scenarios is lower

290   than in Cases (1) and (2). In such situations, the region defined by the candidate leak scenarios

291   is small enough to obtain information related to the leak location.

292   To illustrate the utility of the expected identifiability, a first example is shown in Figure 6. In

293   this figure, the CDF of the expected identifiability is given for two values of the global demand

294   (the demand on the entire network): 830 l/min and 415 l/min. These results are for a leak

295   intensity of 100 l/min and the same sensor configuration shown previously. This graph shows

296   that there is a 95% probability to identify less than 120 candidate leak scenarios (or to falsify

297   more than 145 leak scenarios), for the demand of 415 l/min. This means that in 95% of cases it

298   is possible to reduce the population of candidate leak scenarios by half for a leak intensity of

299   100 l/min. With a 50% probability, it is possible to reduce the initial model set to less than 69

300   candidate leak scenarios. In comparison, for a global demand of 830 l/min, a 95% probability

301 results in 216 candidate models and 136 for a probability of 50%. This graph shows that the

302 identification performance is two times better for the flow rate of 415 l/min because the

303 expected population of candidate models is approximately equal to half when compared to that

304 for the 830 l/min flow rate.

305 The second example shows the expected identifiability when using pressure sensors rather than

306 flow sensors (Figure 7). The model and the parameters are exactly the same as before, with the

307 same associated uncertainties (the global demand is 830 l/min). The only difference is that the

308 pressure at the nodes are predicted instead of the flow in the pipes. In this graph the performance

309 is given for three sensor configurations. They were obtained with a greedy algorithm that

310 optimized the expected identifiability for the 95% probability (Moser et al. 2016a). The

311 configurations are composed of three, five and 15 sensors to show the evolution of performance

312 when increasing the number of sensors. For comparison, the curves of the three flow-sensor

313 configurations are also given.

314 These results show that the increase of the performance when increasing the number of sensors

315 is not very pronounced. This is especially true around the 95% probability where the increase

316 is almost null. By comparing these results with the CDF of the three-sensor configuration, the

317 conclusion can be made that in this specific case, measuring flow is more appropriate than

318 measuring pressure. For three flow sensors, the performance is significantly greater than for 15

319 pressure sensors. The reason is that variations observed in the pressures predictions for leak

320 scenarios are too small in comparison with values for the threshold bounds. Therefore, scenarios

321 cannot be differentiated by pressure predictions. In another situation having lower uncertainty,

322 pressure sensors might be used efficiently. Pressure measurements are more often used with

323 transient models (Whittle et al. 2013).

324 *Demand estimation*

325 In most networks, knowledge regarding the distribution of demand is low. Nevertheless, the

326 global demand is often known. It is computed by measuring the water that goes in and out of

327 the network. Although there are counters for each paying consumer, these counters only record

328 the yearly cumulate consumption; there is no information about how this distribution varies, for

329 example, throughout a day.

330 The behavior of water distribution networks is governed by the demand of the consumer. For

331 this reason, it is important to increase knowledge regarding demand parameters. This can be

332 achieved using error-domain model falsification. The methodology developed for this purpose

333 is illustrated using simulated measurements which are retrieved in the manner described in the

334 methodology section.

335 The methodology is essentially the same as that used for leak detection. The difference is in the

336 identification objectives. The model instances that are used to compute the predictions are

337 different. Instead of leak scenarios, they are built from demand scenarios.

338 Demand scenarios

339 In order to estimate the demand, the model instances are built using the nodal demand as the

340 primary parameter. For this reason, the scenarios are referenced as demand scenarios. Each

341 demand scenario represents a specific demand configuration of the system. In the same way as

342 for the leak scenarios, assumptions have to be made in order to limit the sampling size. It is not

343 possible to sample the demand at each node and then to build all the permutations such that all

344 possible behaviors are explicitly considered. The number of scenarios is equal to the number of

345 nodes as based with an exponent of the number of samples for each node. For example, if three

346 sampling values are tested at each node, then, for a total of 265 nodes, the number of scenarios

347 is greater than 18 million (265^3).

348 In order to achieve consistent sampling, the number of nodes where the demand is estimated

349 needs to be reduced. This is achieved by using a network reduction technique (Moser et al.

350 2015). The reduction is shown in Figure 8. Only nodes at the three monitored pipes and the

351 nodes connected to the tank and reservoir are included in the reduced network. By performing

352 the sampling only at the nodes connected to the monitored pipes, the task of estimating the

353 demand is reduced to six nodes. This is the upper limit for sampling. For eight sampling values

354 at each node, the number of scenarios is greater than 1 million.

355 Generally, the global demand is known or can be estimated. That information can be used for

356 the sampling by adding a constraint that fixes the sum of the six nodal demands to be equal to

357 the global demand. If the global demand is not precisely known, then sampling can be repeated

358 for various global-demand values in the same way that it has been done for leak intensity. For

359 this reason, this parameter is termed demand intensity. In order to build scenarios, the demand

360 intensity is divided by the number of nodes in the non-reduced network. Then, the subdivided

361 demands equivalent to the mean nodal demand, are distributed randomly to each of the six

362 nodes in the reduced network. By doing this, the sum will always remain equal to the demand

363   intensity. In the next section, results using simulated measurements (retrieved in manner

364   presented in the methodology section) to estimate the number of scenarios that need to be built

365   following this procedure in order to have a consistent sampling are presented.

366   Comparison with simulated measurements

367   The EPANET model is run with varying demand. The demand of each node is varied following

368   a time pattern that was built randomly. Figure 9 shows the pattern for Node 1. The horizontal

369   axis gives the time in hours, and the vertical axis gives the nodal demand in l/min. The time

370   step for the pattern is five minutes. The black curve represents the demand for Node 1, and the

371   grey curve represents the total demand (i.e., the sum of the six nodal demands). The demand

372   pattern for the other nodes is not shown.

373   The model of the network is then simulated with these patterns and according to Equation 4.

$$\boldsymbol{y_{sim}(t_j)} = \boldsymbol{h}\left(\theta_1(t_j), \dots, \theta_k(t_j)\right) + \boldsymbol{u}_{combined} \qquad (4)$$

374   Simulated measurements are obtained by taking the flow value prediction. In the same way that

375   it has been done for leak detection (and described at the end of the methodology section), the

376   combined uncertainty is added to the predictions to obtain simulated measurements. Simulated

377   measurements are used to test demand estimation through error-domain model falsification.

378   The uncertainties used are the same as in the leak detection. The only difference is that the

379   uncertainty of the demand is removed, because the demand is the parameter which needs to be

380   identified.

381   Each measurement is compared to the predictions obtained by simulating a population of

382   demand scenarios. Then, after the model falsification process, measurements are associated

383   with a population of candidate demand scenarios. The flowchart in Figure 10 illustrates the

384   process for demand estimation and how to ensure the quality of the sample.

385   Figure 11 shows results obtained when testing the number of samples necessary for the demand

386   estimation. For each sample size tested, the number of times the correct value is included in the

387   candidate models is computed (the percentage of correct identification). The sample sizes tested

388   are 10,000, 20,000, 40,000 and 80,000. The results show that at 40,000 samples, the increase

389   in the six nodes is over 90% and the increase after that slows. The cost of using more than

390   40,000 in terms of computation is drastically larger than the amount of increase in performance

391   which would be achieved.

392 Figure 12 shows the results obtained for the estimation of the demand for the six nodes with
393 40,000 samples. The solid lines (versus the individual points) represent the 95% confidence
394 intervals of the estimation, and the points are the exact demand values to identify. In accordance
395 with previous results, the real value is inside the confidence interval in most cases.

396 **Case studies**

397 In this section, two case studies involving existing water distribution networks are presented.
398 The first case study is part of the water-distribution network of the city of Lausanne. An
399 experimental campaign was carried out to simulate leaks by opening hydrants. The second case
400 study is from a water distribution network of the commune of Bagnes. With this network, a
401 sensor placement study was carried out. These case studies show the potential of error-domain
402 model falsification for the performance assessment of water distribution networks. The aspects
403 covered by each case study are summarized in Table 3.

404 *Lausanne water distribution network*

405 This case study is based on a section of the water distribution network in Lausanne, Switzerland.
406 The water distribution network in the city of Lausanne is separated into six independent
407 subnetworks. This case study is based on an experimental campaign where leaks are created
408 throughout the network at different locations by opening hydrants.

409 The model of this network is shown in Figure 13. It consists of 265 demand-nodes and 295
410 pipes. The pipes are represented by black lines and the nodes, white circles. This network is
411 equipped with three flowmeters. Their positions are given by the black crosses.

412 The goal of this part of the study is to test the error-domain model-falsification methodology
413 through various leak scenarios. These scenarios have been created by opening nine hydrants at
414 four flow rates in order to simulate leaks at each position. The positions of the hydrants have
415 been chosen such that the main regions of the sub-network are covered. They are given by the
416 numbers in circles in the network representation displayed in Figure 13.

417 The flowmeter locations have been chosen using a sensor placement methodology based on the
418 greedy algorithm and expected identifiability (Moser et al. 2016a). All three flowmeters are
419 electromagnetic insertion flowmeters: the HydrINS 2 from hydreka (Figure 14). They have
420 been programmed to take measurements every 15 minutes.

421   The behavior of a water distribution network is often governed by consumer demand.
422   Generally, this data is not readily available. For this study case, the only available information
423   is the global demand of the network. There is no information regarding the distribution of the
424   demand throughout the network. In order to reduce the uncertainty resulting from such a lack
425   of information, measurements are recorded only during the period of the day when consumption
426   is the lowest. This is between 1:00 am and 4:30 am. Figure 15 shows the flow that is measured
427   for one week (9th March to 15th March 2015) during the lowest consumption period.

428   Demand estimation

429   The demand of each node in the network is unknown. In order to bring the model behavior
430   closer to the real behavior, error-domain model falsification is used to estimate the demand in
431   the network. This is done by comparing demand scenarios with measurements. It is assumed
432   that there is no leak in the network at the time of this measurement.

433   The only information available to model demand scenarios is the global demand of the network.
434   It is not possible to use a normal sampling strategy to cover all possible behaviors of the system
435   because the demand of each of the nodes can vary. The result is that the number of scenarios is
436   equal to the number of nodes as a base with an exponent equal to the number of samples for the
437   demand. For three sampling values and 265 nodes there are more than 18 million scenarios.

438   To overcome this challenge, a two-part solution is proposed. The first part of this solution is to
439   obtain a reduced network keeping only the pipes that are monitored (Moser et al. 2015). Then,
440   the demand is modelled only on the nodes connected to the monitored pipes (six nodes for the
441   City of Lausanne network).

442   This leads to the second part of the solution—modelling the demand at the nodes randomly in
443   order to build a number of demand scenarios. This is accomplished by using the only
444   information available: the global demand. The condition is fixed such that the sum of the nodal
445   demands at each node equals the global demand. The demand is allocated to each node by
446   following a discrete uniform distribution varying from zero to the global demand. For this case
447   study, 40,000 samples are used. The results in Figure 11 illustrate that this amount of samples
448   is sufficient. This figure shows that above 40,000 samples, the increase of performance slows
449   down significantly.

450 Figure 16 shows results for the estimation of the demand for the six nodes of the reduced

451 network. In each graph, the horizontal axis represents the time. For this example, the time period

452 is the same used previously to present the measurements. The vertical axis represents the

453 demand for the node, given in l/min. The black curves are the 95% confidence intervals on the

454 demand estimation. This means that, in each plot, 95% of the candidate models are between the

455 two black curves. The dashed black curves display the median of the estimation and the grey

456 curves, the average. The median and the average show that for all nodes except Node 3, the

457 majority of candidate models are concentrated in the lower half of the confidence interval. This

458 means that the estimation of the demand is higher for Node 3.

459 The results also show that the demand varies at each measurement time. In the following

460 section, the demand used for leak detection is the average of the estimation performed the hour

461 before the experiment, assuming that the demand does not vary significantly throughout the

462 experiment. The graphs show that there are periods where the intensity is stable.

463 Leak-region detection

464 As explained previously, in order to test the leak detection methodology, an experimental

465 campaign was carried out. Leaks were simulated on the network by opening hydrants. For each

466 hydrant, four leak intensities were tested: 25 l/min, 50 l/min, 75 l/min and 100 l/min. The

467 procedure was the following. Each night during the campaign, a hydrant was opened. The flow

468 coming out of the hydrant was measured using a flowmeter. Figure 17 shows the setup used for

469 the experiment.

470 The procedure was to open the hydrant to the first intensity (25 l/min) and then increase the

471 flow each 30 minutes. An illustration of the procedure is given in Figure 18. The blue box that

472 is connected to the hydrant is the flowmeter. Two reasons for waiting 30 minutes are that the

473 perturbation needs time to reach the sensors and a minimum of two measurements are needed

474 for each leak intensity (measurements have been taken every 15 minutes, this frequency was

475 chosen to limit the amount of data and has no effect on the accuracy of the estimation). The

476 positions of the nine hydrants used during the experimental campaign are illustrated on the

477 network in Figure 13. Each hydrant is represented by a circle and a number. The hydrants have

478 been chosen to cover all the regions of the sub-network.

479 At first, the results obtained when applying error-domain model falsification with the retrieved

480 measurements show that all models were falsified. While initially alarming, this demonstrates

a strength of error-domain model falsification. This provides a warning that there are wrong assumptions associated with the modelling, sampling and uncertainties. Various reasons can explain such behavior. For example the sampling choice might be inappropriate for the primary parameters.

In this case, the main reason for the falsification of all the models is the way in which the demand of the network has been modeled. Since the distribution of the demand at each node is unknown, it has been modeled as an uncertainty using an exponential distribution as described previously. The results show that this model is too far from reality. For this reason, an estimation of the demand has been carried out using error-domain model falsification. The idea is to use the measurements retrieved before the experiment to estimate the demand during the experiment.

More specifically, the hydrant is opened at 2:15 am with a flow of 25 l/min. The period of time used for the demand estimation is between 1:00 am and 2:15 am. At each measurement time step (every 15 minutes), error-domain model falsification is used to obtain the population of demand scenarios. Each time step is computed separately without considering the transient phenomena. For this reason, only steady-state simulations have been used. Building scenarios considering the time parameters would increase the number of scenarios an exorbitant amount. Then, for each node, the average of the demand is computed for the time period and used as an estimation of the demand for the leak detection. Figure 18 illustrates this procedure.

Threshold estimation

A good estimation of the uncertainty is important for error-domain model falsification. The thresholds used in the methodology are built using uncertainty values. In this case study, the estimation of the modelling uncertainties is difficult because parameters that govern the system behavior, such as the demand, are not well-known.

However, in this case study, the target of the identification is fixed. The leak intensity and location are known. For this reason, the problem is inverted in order to estimate the uncertainties. This is achieved by comparing each measurement to the corresponding prediction. Variations between these values give information about the combined uncertainty of the system.

510   Figure 19 shows the value of measurements and predictions at each step time for two sensors.

511   Measured values are represented by black lines. Predicted values are represented by the short

512   dashed lines for the predictions obtained with demand estimation and long dashed lines for

513   predictions obtained without demand estimation. These graphs show that when the demand is

514   modeled with an exponential law instead of estimating it through model falsification, there is a

515   significant bias for the flow in sensor 1. The results for sensor three shows that the curve of

516   predicted values with demand estimations follows the measured values even when there is a

517   jump in the measured values such as between the two tests presented in Figure 19.

518   In order to estimate the combined uncertainty, the differences between each measurement and

519   corresponding predictions are computed. Figure 20 shows these results for the three sensors and

520   for the cases when the demand is estimated and when it is not. The results are provided for the

521   nine hydrant tests, listed on the horizontal axes. The vertical axes give the difference between

522   the measured and predicted flows (in l/min). For each hydrant test, this difference is computed

523   for eight measurements, two per leak intensity. The corresponding points are represented by the

524   black squares on the graphs. The variation of the points across one hydrant test is due to

525   modelling and measurement errors. Maximum and minimum values define an interval that can

526   be considered as an estimation of the uncertainty. The evolution of this interval is illustrated on

527   the graphs by the two grey curves.

528   The results in Figure 20 illustrate that the combined uncertainties are biased. Comparing the

529   results obtained with and without demand estimation shows that estimation of the demand

530   reduces the bias, especially for the first sensor. This demonstrates that estimating the demand

531   will increase the quality of the flow predictions.

532   As explained previously, the demand is estimated before each hydrant test. The evolution of

533   the bias with the hydrant tests shows that the quality of the demand estimation changes from

534   one test to another. This is due to the fact that in some cases the demand changes faster than the

535   estimated value.

536   The results in Figure 20 give the estimation of the uncertainties for each hydrant test separately.

537   Each uncertainty estimation is related to a given demand estimation. Instead of considering

538   each hydrant test individually, the difference between measurements and predictions can be

539   considered together. This results in an estimation of uncertainties that include the uncertainty

540   of the demand estimation process. Figure 21 shows these results in the form of histograms. The

541   horizontal axes represent the difference between predictions and measurements. The vertical

542   axes display the probability. The width of the base of the histogram is a consequence of the

543   variations values, including biases observed in Figure 20.

544   Estimations of uncertainties obtained in this way could be used directly to build thresholds for

545   error-domain model falsification. However, in this case study knowledge of the demand must

546   be enhanced in order to reduce the width of global combined uncertainties.

547   Figure 22 shows the results obtained for a simulated leak (simulated in the model) of 100 l/min

548   when using threshold bounds estimated using all the hydrant tests. These results show that when

549   demand estimation is used with threshold bound determination it is possible to identify the leak

550   region.

551   *Bagnes water distribution network*

552   This case study is based on one of the water distribution networks of Bagnes. Bagnes is a

553   commune in Valais State (Switzerland), situated in the mountains. Bagnes is made up of many

554   villages, the most famous being Verbier. The water distribution networks of Bagnes are

555   monitored in order to help with management of the networks. Each network in Bagnes is

556   connected to one or more tanks that supply the water. The water going in and out of each tank

557   is monitored continuously in order to directly gain knowledge of the consumption of each

558   network.

559   This data can be used to detect leaks by observing abnormal variations in the measurements.

560   However, the information is not sufficient to locate the leak-region, especially for networks

561   connected to only one tank. This case study will initiate with a leak that has been observed and

562   show the gain that can be obtained by installing sensors throughout the network.

563   Figure 23 shows the model of the water distribution network of Bagnes. It is made up of 900

564   nodes and 904 pipes. In comparison with the water distribution network of Lausanne shown

565   previously, the number of pipes and nodes seems high. It is not because this network is bigger;

566   in terms of size, it is a smaller network. The reason for the higher number of pipes and nodes is

567   that the representation is more refined for the model of Bagnes. In the case of the Lausanne

568   network, the network is already simplified.

569   The advantage of working on a smaller network is that the lowest consumption value is smaller.

570   Since Lausanne is a city, even during nights, there are activities that take water from the

571   network. For the Lausanne network the lowest consumption is around 830 l/min. For this

network, the lowest consumption is approximately 100 l/min. This data is displayed on Figure 24 which shows the mean hourly consumption for the month of August. The challenge is not the same in winter because this network is in the village of Verbier, one of the more prominent ski resorts in Switzerland. In winter, the population of Verbier increases to 50,000 inhabitants although it counts only 3,000 official inhabitants. This means that in winter the consumption, as well as the related uncertainty, is higher.

During the summer of 2013, a jump was observed in the flow measurement that records the water coming into the network from the tank. This jump is illustrated in Figure 25. This graph compares the daily measurements taken between the 21st of July and the 24th of September in 2012 and 2013. The jump measured in 2013 is due to a leak. Using this measurement, the leak intensity is estimated to be 200 l/min. These measurements also show that the leak was active for approximately 15 days. That means that it took more than 10 days to detect, locate and repair the leak. That time could be significantly reduced by using a monitoring system for leak detection. This amount of time with such a leak represents a loss of more than 4 million liters of fresh water. This study will show that by using error-domain model falsification, the leak-region can be located.

Leak-region detection

In this section, the leak detection methodology is tested for the leak that occurred in 2013. In order to achieve this, the same leak is simulated. The simulation of the leak is used to build simulated measurements. These measurements are then treated with error-domain model falsification for three sensor configurations: one with two sensors (Figure 26), one with six sensors (Figure 27, top) and one with ten sensors (Figure 27, bottom). The locations of the sensors are given by the black crosses. The nodes in dark represent the candidate leak scenarios. The position of the leak is shown by the four arrows.

The graph in Figure 28 shows the predicted value for the sensor in the middle of the branch where the leak is located (the sensor is represented above the graph). The horizontal axis gives the leak scenarios and the vertical axis, the predicted flow. The predictions are represented by the black points. The dashed horizontal lines are the threshold bounds and the continuous line, the value of the simulated measurement. All the points that are not between the thresholds are falsified. This figure clearly shows that in this case this sensor configuration is sufficient to identify the leak region.

603	**Conclusions and discussion**

604 An error-domain model-falsification methodology that is uniquely adapted for leak-region
605 detection demonstrates potential for practical use.

606 Error-domain-model falsification is useful for estimating the demand at a small number of
607 nodes. The strategy to estimate combined uncertainty helps aggregate uncertainty sources.

608 The study of the Lausanne network revealed that demand estimations decrease the uncertainty
609 of the system and lead to better performance for leak detection. The estimation of uncertainties
610 shows that significant bias is present. This supports the use of error-domain model falsification
611 for data interpretation. Demand estimation removes part of the systematic uncertainty.
612 Reducing systematic uncertainty lowers interdependence of measurement locations, and this
613 improves predictions.

614 The results of the Bagnes case study further show that error-domain model falsification can
615 help locate leak regions within a water supply network. This is demonstrated through the
616 example of a leak that has occurred on the Bagnes network. This example shows that even high
617 intensity leaks take time to be located without such support for the leak detection, and this
618 results in significant water loss.

619 In addition, this case study shows that a smaller network, situated in a village rather than a city,
620 could have a smaller minimum demand ratio, and thus reduced uncertainty.

621 In all of the case studies presented in this paper, the networks were dependent on a single reservoir or
622 tank. In reality, networks can be designed in various ways, including, for example, with intermediate
623 reservoirs. The methodology presented is capable of accommodating such networks. The manner in
624 which the network is modelled would need to include these new parameters.

629 **References**

630

631 ADEC, (1999). *Technical review of leak detection technologies - vol. 1 - crude oil transmission pipeline.* Vol. 1.
632 1999, Alaska: Alaska Department of Environmental Conservation.

633 Andersen, J.H. and Powell, R.S. (2000). Implicit state-estimation technique for water network monitoring, *Urban*
634 *Water, 2*(2): p. 123-130.

635 Babbitt, H., Amsbary, F. and Gwinn, D. (1920). The detection of leaks in underground pipes, *Journal (American*
636 *Water Works Association), 7*(4): p. 589-595.

637 Barandouzi, M. A., Mahinthakumar, G., Brill, E. D. and Ranjithan, R. (2012). "Probabilistic Mapping of Water
638 Leakage Characterizations Using a Bayesian Approach," in *Proceedings of World Environmental and Water*
639 *Resources Congress 2012*, Albuquerque, New Mexico, USA. 3248-3256. ASCE.

640 Box, G.E. and Draper, N.R. (1959). A basis for the selection of a response surface design, *Journal of the American*
641 *Statistical Association, 54*(287): p. 622-654.

642 Colombo, A.F., Lee, P. and Karney, B.W. (2009). A selective literature review of transient-based leak detection
643 methods, *Journal of Hydro-environment Research, 2*(4): p. 212-227.

644 Demirci, S., Yigit, E., Eskidemir, I. H. and Ozdemir, C. (2012). Ground penetrating radar imaging of water leaks
645 from buried pipes based on backprojection method, *NDT & E International, 47*(0): p. 35-42.

646 Fang, H., Rais-Rohani, M., Liu, Z. and Horstemeyer, M.F. (2005). A comparative study of metamodeling methods
647 for multiobjective optimization, *Computers and Structures, 83*(25-26): p. 2121-2136.

648 Gao, Y., Brennan, M.J. and Joseph, P.F. (2006). A comparison of time delay estimators for the detection of leak
649 noise signals in plastic water distribution pipes, *Journal of Sound and Vibration, 292*(3–5): p. 552-570.

650 Gao, Y., Brennan, M.J. and Joseph, P.F. (2012). On the effects of reflections on time delay estimation for leak
651 detection in buried plastic water pipes, *Journal of Sound and Vibration, 325*(3): p. 649-663.

652 Goulet, J. and Smith, I.F.C. (2012). Performance-driven measurement system design for structural identification,
653 *Journal of Computing in Civil Engineering, 27*(4): p. 427-436.

654 Goulet, J.-A. and Smith, I.F.C. (2013). Structural identification with systematic errors and unknown uncertainty
655 dependencies, *Computers & structures, 128*: p. 251-258.

656 Goulet, J., Coutu, S. and Smith, I.F.C. (2013). Model falsification diagnosis and sensor placement for leak
657 detection in pressurized pipe networks, *Advanced Engineering Informatics, 27*(2): p. 261-269.

658 Grunwell, D. and Ratcliffe, B. (1981). "Location of underground leaks using the leak noise correlator," in *WRC*
659 *Technical Report*. 1981, WRC.

660 Hope, W. (1892). The waste of water in public supplies and its prevention, *Minutes of the Proceedings 110,* 260-
661 275.

662 Johnson, D.W. (1947). Losses in Distribution Systems. *Journal (American Water Works Association), 1947:* p.
663 157-167.

664 Lambert, A. and Hirner, W. (2000). "Losses from water supply systems: standard terminology and recommended
665 performance measures," in *the blue pages the IWA information source on drinking water issues*, 2000.

666 Mergelas, B. and Henrich, G. (2005). Leak locating method for precommissioned transmission pipelines: North
667 American case studies, *Leakage 2005*, p. 12-14.

668 Morrison, J. (2004). Managing leakage by district metered areas: a practical approach, *Water 21,* 2004(IWA Task
669 Force): p. 44-46.

670 Moser, G., Paal, S.G. and Smith, I.F.C. (2015). Performance comparison of reduced models for leak detection in
671 water distribution networks, *Advanced Engineering Informatics, 29*(3): p. 714-726.

672 Moser, G., Paal, S.G., Jlelaty, D. and Smith, I.F.C. (2016a). An electrical network for evaluating monitoring
673 strategies intended for hydraulic pressurized networks, *Journal of Advanced Engineering Informatics, 30* (4): pp.
674 672-686.

675 Moser, G. Paal, S.G. and Smith, I.F.C. (2016b). Measurement system design for leak detection in hydraulic
676 pressurized networks, *Structure and Infrastructure Engineering*, DOI: 10.1080/15732479.2016.1225312, 30 Aug
677 2016.

678 Mounce, S., Boxall, J. and Machell, J. (2009). Development and verification of an online artificial intelligence
679 system for detection of bursts and other abnormal flows, *Journal of Water Resources Planning and Management,*
680 *136*(3): p. 309-318.

681 Mounce, S.R., Mounce, R.B. and Boxall, J.B. (2011). Novelty detection for time series data analysis in water
682 distribution systems using support vector machines, *Journal of hydroinformatics, 13*(4): p 672-686.

683 Murray, P.S. and Silea, I. (2012). A survey on gas leak detection and localization techniques, *Journal of loss
684 prevention in the process industries,* 2012.

685 Niemeyer, H. (1940). Leak Detection, *Journal (American Water Works Association), 1940*: p. 1354-1358.

686 Pasquier, R. and Smith, I.F.C. (2015). Robust system identification and model predictions in the presence of
687 systematic uncertainty, *Advanced Engineering Informatics.*

688 Poulakis, Z., Valougeorgis, D. and Papadimitriou, C. (2003). Leakage detection in water pipe networks using a
689 Bayesian probabilistic framework, *Probabilistic Engineering Mechanics, 18*(4): p. 315-327.

690 Pudar, R.S. and Liggett, J.A. (1992). Leaks in Pipe Networks, *Journal of Hydraulic Engineering, 118*(7): p. 1031-
691 1046.

692 Puust, R., Kapelan, Z., Koppel, T. and Savic, D. (2006). "Probabilistic Leak Detection in Pipe Networks Using
693 the SCEM-UA Algorithm", in *Proceedings of Water Distribution Systems Analysis Symposium 2006*, Cincinnati,
694 Ohio, USA. 1-12. ASCE.

695 Puust, R., Kapelan, Z., Savic, D.A. and Koppel, T. (2010). A review of methods for leakage management in pipe
696 networks, *Urban Water Journal, 7*(1): p. 25-45.

697 Robert-Nicoud, Y., Raphael, B. and Smith, I.F.C. (2005). Configuration of measurement systems using Shannon's
698 entropy function, *Computers and Structures, 83*(8): p. 599-612.

699 Romano, M., Kapelan, Z. and Savić, D.A. (2012). Automated detection of pipe bursts and other events in water
700 distribution systems, *Journal of Water Resources Planning and Management, 140*(4): p. 457-467.

701 Romano, M., Kapelan, Z. and Savić, D.A. (2013). Geostatistical techniques for approximate location of pipe burst
702 events in water distribution systems, *Journal of hydroinformatics, 15*(3): p. 634-651.

703 Romano, M., Kapelan, Z. and Savić, D.A. (2014). Evolutionary Algorithm and Expectation Maximization
704 Strategies for Improved Detection of Pipe Bursts and Other Events in Water Distribution Systems, *Journal of
705 Water Resources Planning and Management, 140*(5): p. 572-584.

706 Rossman, L.A. (2000). *EPANET 2: users manual, Cincinati, OH: US Environmental Protection Agency.*

707 Rougier, J. (2005). Probabilistic leak detection in pipelines using the mass imbalance approach, *Journal of
708 Hydraulic Research, 43*(5): p. 556-566.

709 Senus, (2012). *Water 20/20: Bringing smart water networks into focus.* Technical report, 2012.

710 Smith, I.F.C. (2016). Studies of Sensor Data Interpretation for Asset Management of the Built Environment,
711 *Journal of Frontiers in Built Environment, 2:*8.

712 Srirangarajan, S., Allen, M., Preis, A., Iqbal, M., Lim, H. B. & Whittle, A. J. (2010). "Water main burst event
713 detection and localization", in *Proceedings of Proceedings of 12th Water Distribution Systems Analysis
714 Conference (WDSA'10).*

715 Vítkovský, J. P., Simpson, A. R. & Lambert, M. (2000). Leak detection and calibration using transients and genetic
716 algorithms, *Water Resources Planning and Management*, 258–262.

717 Vítkovský, J. P., Lambert, M. F., Simpson, A. R. & Liggett, J. A. (2007). Experimental observation and analysis
718 of inverse transients for pipeline leak detection, *Journal of Water Resources Planning and Management,* 133, 519.

719 Whittle, A. J., Girod, L., Preis, A., Allen, M., Lim, H. B., Iqbal, M., Srirangarajan, S., Fu, C., Wong, K. J. &
720 Goldsmith, D. (2010). WATERWISE@ SG: A testbed for continuous monitoring of the water distribution system
721 in singapore, *Water Distribution System Analysis, WSDA.*

722 Whittle, A., Allen, M., Preis, A. & Iqbal, M. 2013. "Sensor Networks for Monitoring and Control of Water
723 Distribution Systems", in *Proceedings of The 6th International Conference on Structural Health Monitorinf of
724 Intelligent Infrastructure*, Hong Kong.

725

726 Table 1. Uncertainties related to secondary parameters (Exp is an exponential distribution, N is Gaussian and U
727 is uniform). The arguments of the distribution contain defining parameters.

Parameter	Uncertainty distribution
Nodal demand [l/min]	$\sim Exp(1/3.13)$
Node elevation [m]	$\sim N(0,0.015)$
Pipe diameter [mm]	$\sim N(0,0.75)$
Pipe length [m]	$\sim U(-0.03,0.07)$
Pipe roughness	$\sim U(0,0.015)$
Tank level [m]	$\sim N0(0,0.32)$

728

729 Table 2. Relative importance of secondary-parameter uncertainties

Parameter	Relative importance for flow predictions [%]	Relative importance for pressure predictions [%]
Nodal demand [l/min]	99.77	97.81
Node elevation [m]	5.45E-04	9.06E-02
Pipe diameter [mm]	2.25E-01	5.14E-01
Pipe length [m]	3.11E-03	3.34E-02
Pipe roughness	5.34E-05	1.49
Tank level [m]	2.80E-04	6.38E-02

730

731 Table 3. Overview of aspects covered by each case study

Case study	Aspect illustrated				
	Leak detection	Demand estimation	Uncertainty estimation	Network reduction	Sensor placement
Lausanne network	✓	✓	✓		
Bagnes network	✓			✓	✓

732

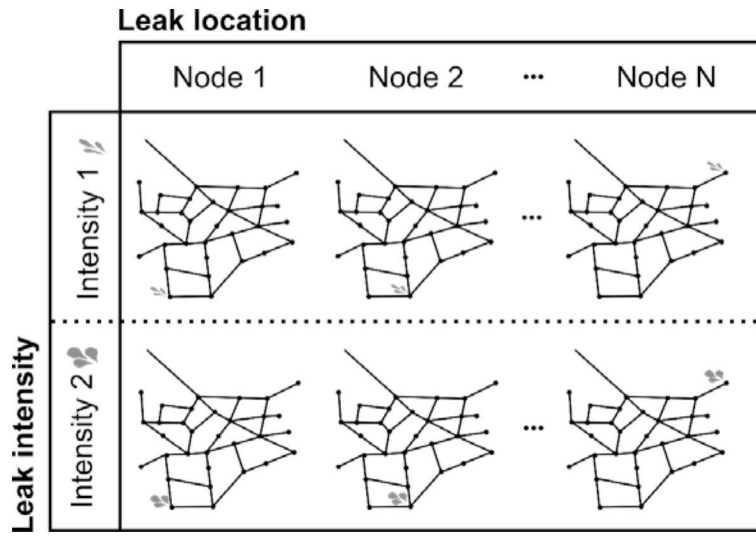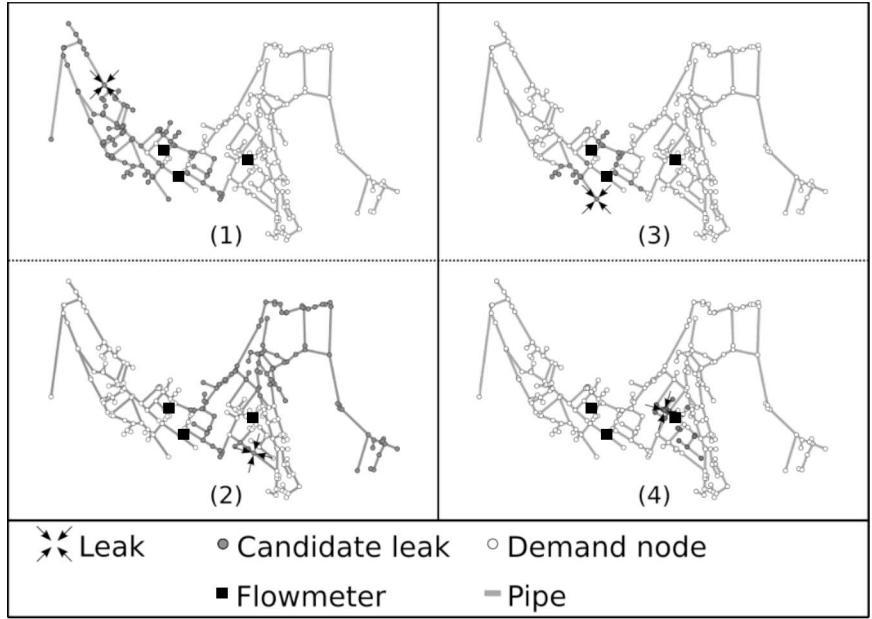## Leakage rates by country [%]

Country	Rate
Bangladesh	48
Mexico	45
Brazil	39
China	36
Saudi Arabia	35
South Africa	29
France	27
United Kingdom	21
Average	20
Russia	19
Australia	18
India	18
United States	11
Germany	7
South Korea	5

Numerical model

Model instance generation

Scenarios: $s_i = [\Theta_{i1}, ..., \Theta_{ik}]$

$\begin{pmatrix} \Theta_{ik} \text{ parameter k for} \\ \text{scenario i} \end{pmatrix}$

Model **g( )**

Predictions: $g_i = g(\Theta_{i1}, ..., \Theta_{ik})$

Comparison with simulated measurements
(prior to measurement)

Model instances   Simulated measurements

Error-domain model-falsification

Candidate models ➡ Predicted performance

Comparison with measurements

Comparison

y

$g_i , \; i = 1, ..., n$

Candidate models

Falsified models

if $\quad T_{low} \leq \; g_i - y \; \leq T_{high}$

$\Longrightarrow g_i$ is a candidate model

Physical model

Water-distribution network

Measurements y

Numerical model

Model instance generation

Scenarios: $\boldsymbol{s}_i = [\Theta_{i1}, ..., \Theta_{ik}]$

$\begin{pmatrix} \Theta_{ik} \text{ parameter k for} \\ \text{scenario i} \end{pmatrix}$

Model $\boldsymbol{g()}$

Predictions: $\boldsymbol{g}_i = \boldsymbol{g}(\Theta_{i1}, ..., \Theta_{ik})$

Comparison with measurements

$\boldsymbol{y}$

Comparison

$\boldsymbol{g}_i, \ i = 1, ..., n$

Corresponding model

Error = Predictions - Measurments

$\boldsymbol{g}$ $\qquad \boldsymbol{y}$

Uncertainty estimation

Probability

Error

Physical model

Measurements $\boldsymbol{y}$

Water-distribution network

Scenario

Leak location

	Node 1	Node 2	···	Node N
Intensity 1			···	
Intensity 2			···	

Leak intensity

(1)

(3)

(2)

(4)

Leak   ● Candidate leak   ○ Demand node

■ Flowmeter   — Pipe

Figure: Cumulative Probability versus Number of candidate leak scenarios for 3 Flow sensors, 3 Pressure sensors, 5 Pressure sensors, and 15 Pressure sensors. An arrow labeled "Total number of candidate leak scenarios" points to 265.

Start

Model instance generation

Input :   n demand-scenarios

$$s_i = [\Theta_{i1}, ..., \Theta_{ik}]$$

$$\left(\begin{array}{c}\Theta_{ik} \text{ demand at node } k \\ \text{for scenario } i\end{array}\right)$$

EPANET model $g(\ )$

Output :   Flow predictions

$$g_i = g(\Theta_{i1}, ..., \Theta_{ik})$$

Simulated measurement generation

Input :   nodal-demand
time pattern

$$[\Theta_1(t), ..., \Theta_k(t)]$$

$$\left(\begin{array}{c}\Theta_k(t) \text{ demand at node } k \\ \text{at time } t\end{array}\right)$$

EPANET model $h(...,t)$
+ combined uncertainties

Output :   Simulated flow measurements

$$y_{sim}(t_j) = h\left(\Theta_1(t_j), ..., \Theta_k(t_j)\right) + u_{combin}$$

**Comparison of simulated
measurements y
with model instance predictions g_i**

For each time step j
if

$$T_{low} \leq \ g_i - y \ \leq T_{high} \ , i = 1, ..., n$$

$\Longrightarrow$ g_i is a candidate model

**Increase number of
samples or change
sampling strategy**

Results

- Nodal demand
- Demand estimation
  ranges
  (95% conf. interval)

Performance: percentage of nodal demand
point inside demand
estimation ranges

No

Is state
criteria
reached
?

Yes

End

10

Node 1

Node 2

Node 3

Node 4

Node 5

Node 6

■ Time nodal demand

▬ Demand estimation ranges
(95% confidence interval)

Pipe

Flowmeter

Measurment time

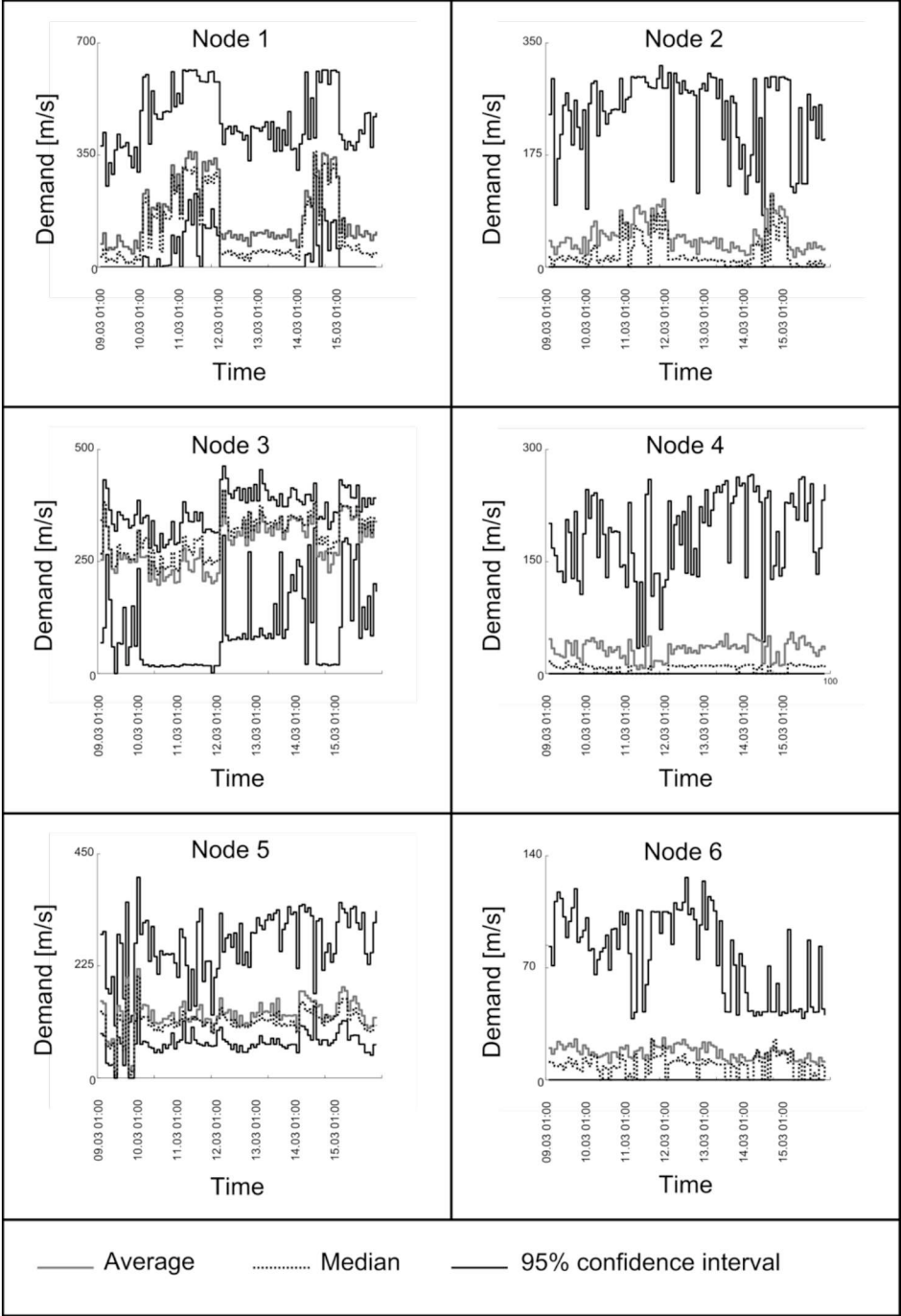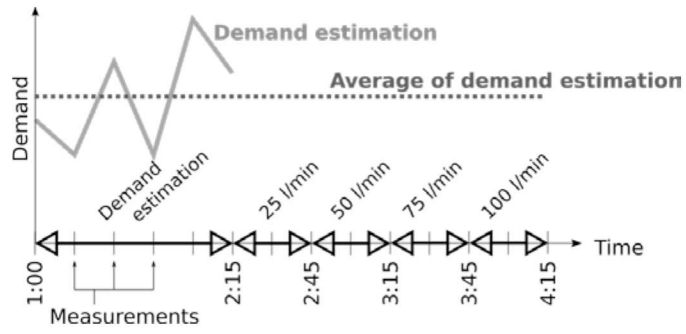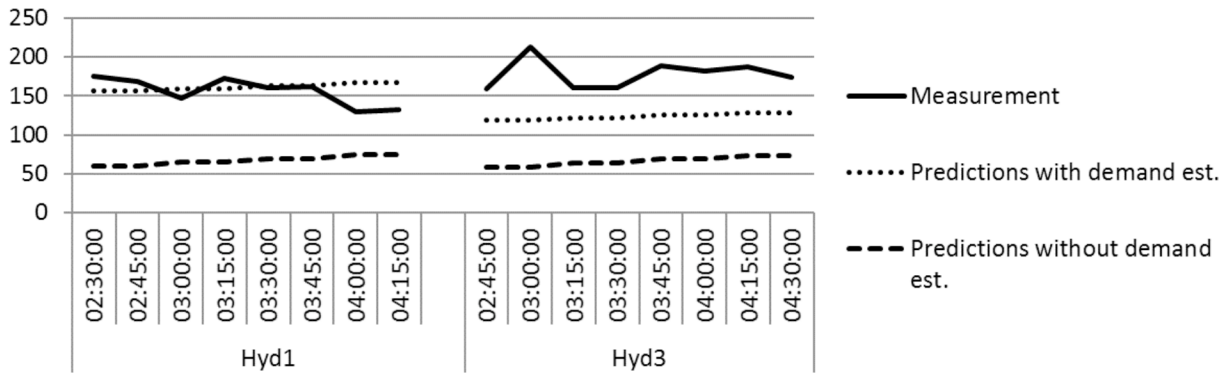Node 1 — Node 6 plots of Demand [m/s] vs Time, showing Average, Median, and 95% confidence interval.

Hydrant

Flowmeter

Sensor 1

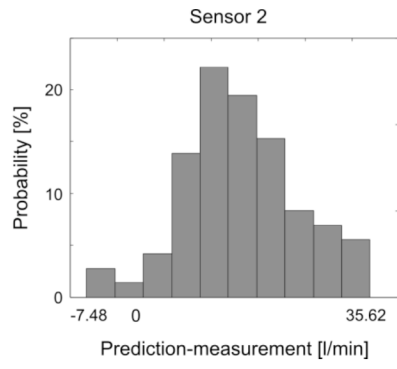## Sensor 3

With demand estimation   **Without demand estimation**

Sensor 1

Sensor 2

Sensor 3

Max(Pred-Meas)
Min(Pred-Meas)
♦ Pred-Meas

20

Sensor 1

Sensor 2

Sensor 3

| ✳ Leak | ● Candidate leak | ○ Demand node |
| □ Sensor | ▬ Pipe | |

Pipe
Junction
Tank
Flowmeter

Hourly consumption

Y-axis: Consumption [l/min] — 0, 50, 100, 150, 200, 250, 300

X-axis: Hours — 01:00, 02:00, 03:00, 04:00, 05:00, 06:00, 07:00, 08:00, 09:00, 10:00, 11:00, 12:00, 13:00, 14:00, 15:00, 16:00, 17:00, 18:00, 19:00, 20:00, 21:00, 22:00, 23:00, 00:00

Lowest consumption

— Hourly consumption